Shearing transition in a superconducting vortex lattice subject to periodic pinning

Y. J. Rosen,[1,2,3] S. Guénon,[3] and Ivan K. Schuller[3]
[1]*Laboratory for Physical Sciences, College Park, Maryland 20740, USA*
[2]*Department of Physics, University of Maryland, College Park, Maryland 20742, USA*
[3]*Department of Physics and Center for Advanced Nanoscience, University of California San Diego, La Jolla, California 92093 USA*
(Received 16 August 2013; revised manuscript received 29 October 2013; published 15 November 2013)

We have studied the shearing forces in a superconducting vortex system with artificial pinning sites using the Corbino geometry. Current was injected into the center of a Nb disc and propagated radially outward to produce a force in the azimuthal direction on the vortices, with strength proportional to $1/r$. We investigated the magnetoresistance properties of the vortex lattice as a function of temperature, current, and pinning lattice configuration. The measurements show steps instead of minima at the matching field positions, indicating an unexpected influence of the pinning array on the motion of the vortex lattice. The results imply that these steps are due to a shearing transition of the vortices.

DOI: 10.1103/PhysRevB.88.174511 PACS number(s): 74.25.Wx, 74.25.Uv, 62.20.−x, 74.78.−w

I. INTRODUCTION

Superconducting vortices provide an ideal method for studying periodic systems moving in the presence of a periodic potential. Similar periodic systems also appear in neutron stars,[1] electron plasmas,[2] droplets on vibrating liquids,[3] etc. Superconducting vortices allow us to study the rich phases seen in periodic systems, including liquid and glass phases,[4,5] ordered periodic lattices,[6] and avalanche effects.[7,8] Interesting effects have also been engineered and simulated in these systems including flux transistors,[9] rectification effects,[10] and jamming transitions.[11]

Using the Corbino geometry,[12] we can examine the shearing forces on a vortex lattice. In this geometry, current enters a superconducting disc at the center and flows radially outward in all directions. The current density in this geometry decreases as $1/r$, where r is the distance away from the center of the disc. The radial current density produces a tangential force on the vortices, which can cause them to rotate in concentric circles. Several vortex phases have been predicted and measured in this geometry, including elastic to laminar flow transitions,[13,14] rectification due to a single flow channel,[15] energy states related to vortex shell configurations,[16] and irreversible flow transitions.[17]

In this paper, we explore the effects of pinning sites on the vortex dynamics in the Corbino geometry. When the shearing forces produced by the current are large, the lattice is in the laminar state, in which each ring can rotate at different angular velocities.[13] However, when the shearing force is small compared to the lattice elastic force, the lattice rotates as a rigid body. In this state, the outer regions of the lattice rotate faster than the regions closer to the center. Adding periodic pinning sites in this configuration adds an additional stress to the lattice due to the difference between the speeds of the vortices. We show that a sudden transition in the resistance occurs due to this stress when the vortex lattice is commensurate with the pinning lattice. We explore this transition as a function of temperature, current, and magnetic fields.

II. EXPERIMENT

The Corbino geometry was fabricated using a five step lithographic process. In the first step, electron-beam lithography was used to pattern a pinning array of dots on a Si substrate. The pinning sites were made of 40-nm-thick Co in order for the magnetic material to increase the pinning effects.[18] Each site was 250 nm in diameter with a total array radius of 30 μm. Two different pinning array geometries were used for this study: a square array [Fig. 1(a)] and a triangular array. Both arrays had a density of 6.25 sites/μm^2. An empty Corbino disc was also measured for comparison.

Once pinning sites were placed on the substrate, a 100-nm-thick Nb layer was deposited on top. The Nb was patterned into a Corbino disc with a radius of 50 μm using photolithography and liftoff technique. The samples had a T_C of approximately 8 K, defined according to the 90% normal resistance criterion.

Au contacts with a thickness of 90 nm were placed on the Corbino disc with a 10 nm Ti adhesion layer on top [the red area in Fig. 1(b)]. The Au contacts were patterned so that current paths leaving the disc were equidistant. Since the resistance of the superconductor is much smaller than the Au, the current path is determined not only by the contact pad shape but also by the leads leaving the current pads. We therefore chose small contact pads in order to achieve better control of the current path. In doing so, we sacrificed some radial symmetry on the edges of the disc; however, radial symmetry was mostly preserved below a 30 μm radius.

In the fourth lithography step, we deposited an insulating SiO_2 disc, 170 μm in radius and 80 nm in thickness, centered on the Corbino disc. Contacts were made by patterning three holes into the SiO_2 [Fig. 1(c)]: one current tap (denoted by I_+) at the center of the disc with radius 5 μm and two square voltage taps with edge length 3 μm placed at distances 17.5 μm (V_1) and 31.5 μm (V_2) from the center. In this geometry, current can enter through the center contact, I_+, flow radially outward, and exit through the outer contacts, I_-. Contacts V_1 and V_2 are used for voltage measurements. A final layer of lithography is used to deposit 100 nm of Au to contact the holes in the SiO_2 and the I_- layer. Our geometry is designed to reduce the amount of insulating SiO_2 area needed to decrease the probability of pinholes.

Magnetoresistance measurements were conducted in a variable temperature liquid-He flow cryostat with temperature stability better than 1 mK. The resistance was measured using a current source and nanovoltmeter in DC polarity

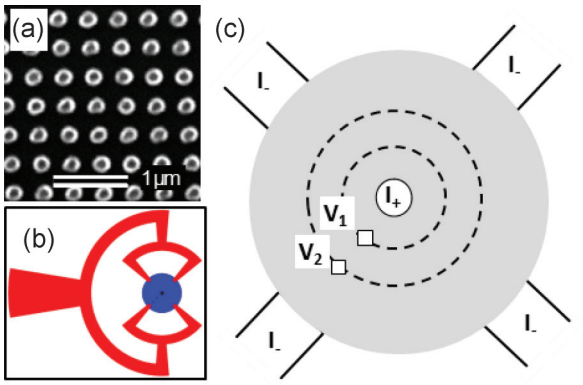

FIG. 1. (Color online) Geometries used for the fabrication of the Corbino system. (a) SEM image of a square array of Co pinning sites. (b) A schematic of the outer Au contacts (red) connected to the Nb Corbino disc (blue). (c) A schematic of the Corbino disc. Current enters through the center (I_+) and leaves from the edges (I_-). The voltage taps are placed at positions V_1 and V_2 at radii 17.5 μm and 31.5 μm, respectively, allowing measurements of the middle ring and the inner region of the disc (dashed lines are added as a guide to the eye).

reversal mode.[19] In this mode, the current oscillates in a square wave pattern at approximately 2 Hz. The current source automatically triggers the voltage probe in order to reduce the noise and voltage drift. The magnetic field was controlled using a Cryomagnetics, Inc. 4G superconducting magnet power supply with a precision of ± 1 Gauss.

III. RESULTS

The Corbino geometry allowed us to investigate two main areas [Fig. 1(c)]: a middle ring, between the V_1 and V_2 voltage contacts, and the inner region, between the V_1 and I_+ contacts. The outer area was disregarded because it does not have a radial current distribution. Measurements of the middle ring were performed in the four-point current/voltage configuration at $I = 10$ μA and with a variety of temperatures [Fig. 2(a)]. The resistance shows the standard matching minima, consistent in position with those seen with a uniform current density.[20] Figure 2(b) shows magnetoresistance measurements of the inner region measured in a three-point configuration at $I = 10$ μA. In this configuration, current is passed between the I_+ and I_- contacts, and voltage is measured over the V_1 and I_+ contacts. In this measurement configuration, the lead resistance is included in the results. The inset of Fig. 2(b) shows the resistance versus temperature curve at zero magnetic field. The resistance has a sharp decrease at T_C, but, unlike the middle ring, the resistance continues to decrease slightly even at low temperatures.

The T_C is defined as the temperature at which the transition has decreased the resistance to 90% of the normal resistance. T_Cs for the magnetoresistance curves in the inner region were calculated from the resistance versus temperature graphs by treating the minimum resistance measured as the resistance of the contacts. This number is not entirely accurate since we were not able to go to the minimum value of the transition. However, the error is small because close to T_C the resistance changes by 1 ohm/20 mK.

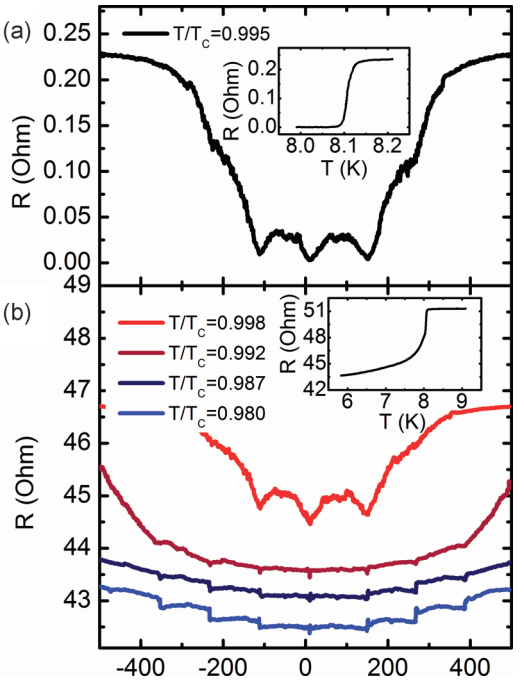

FIG. 2. (Color online) Magnetoresistance of a square array of pinning sites with $I = 10$ μA in different configurations. (a) Measurements of the middle ring of the Corbino disc. Voltage was measured between the V_1 and V_2 leads. (b) Measurements of the inner region of the Corbino disc. Voltage was measured between the I_+ and V_1 leads. The insets show the resistance versus temperature at zero magnetic field.

The magnetoresistance curves shown in Fig. 2 were measured at $T/T_C = 0.998$, 0.992, 0.987, and 0.980. The top curve, measured at the highest temperature, shows minima at the same fields seen in the middle ring. As the temperature is decreased, the amplitude of the minima becomes small and narrow. As the temperature continues to decrease, the minima change into steps occurring at the matching fields with plateaus in between those fields. The same features were present in the triangular sample but not in the sample without a pinning array.

Figure 3(a) shows the height of the step as a function of temperature for different matching fields. As the temperature is reduced, the step height increases. A general trend is observed for the different samples where the step at the first matching field is smaller than the steps at the second and third matching fields.

Figure 3(b) shows the voltage versus magnetic field at two different currents for a square lattice. The step heights are within a factor of two in the voltage scale, even though the current was changed by a factor of 10. Current versus voltage measurements were attempted below and above the steps, however, there was too much noise and drift in the voltage meter.

The steps in the resistance were explored for different magnetic fields in Fig. 4. The field was changed in small increments around the second matching field to determine the properties of the step. Figure 4(a) shows the resistance measured as a function of time while the magnetic field, shown in Fig. 4(b), was varied. When the field was below 264 Oe (shown in blue), the resistance measured was consistently at

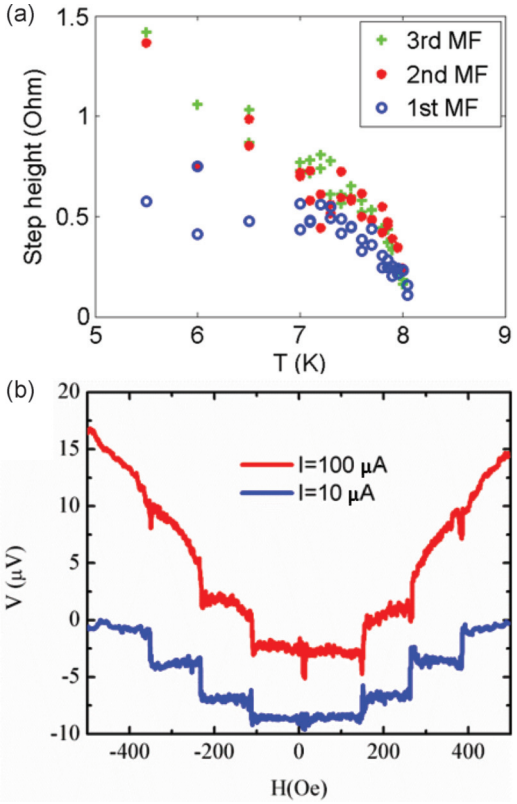

FIG. 3. (Color online) Temperature and current dependencies of the steps. (a) The height of the steps as a function of temperature for a triangular pinning lattice with $T_C = 8.1$ K. Symbols correspond to different matching fields (MF), as indicated by the legend. (b) Voltage as a function of magnetic field for different currents in a square pinning lattice at $T = 7.5$ K. The curves have been shifted along the y axis for clarity.

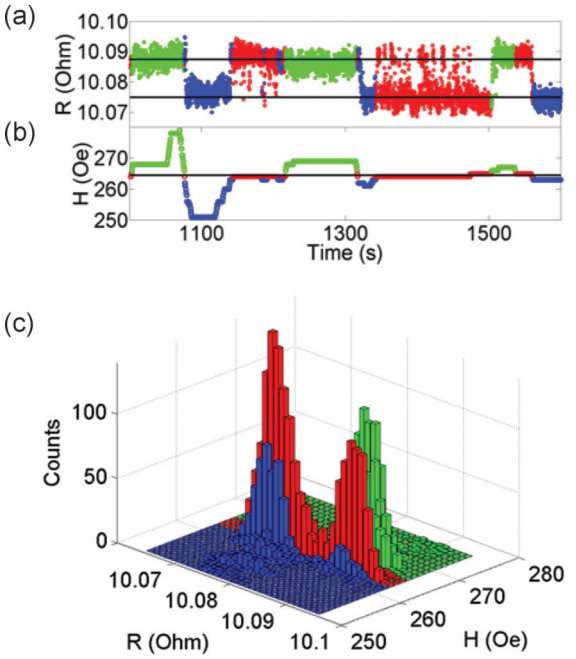

FIG. 4. (Color online) (a) Resistance as a function of time for different magnetic fields. The black lines are a guide to the eye. (b) The field on the sample at the different times. The black line at $H = 264.5$ Oe is a guide to the eye to denote the approximate transition field. (c) Histogram of the number of counts for each resistance and field. In the above graphs, for fields above 265 Oe, the points are shown in green, below 264 Oe the points are shown in blue, and for fields between 264 and 265 the points are shown in red.

the bottom of the step. When the field was above 265 Oe (shown in green), the resistance was consistently at the top of the step. At the transition, the resistance showed a median value that was either at the top of the step or at the bottom of the step but never in between. When the magnetic field was stabilized on the step, the resistance occasionally showed an increase in noise in the direction of the opposing step value. There was no hysteresis measured in the transition to within 1 Oe.

Figure 4(c) shows a histogram of the number of counts for each resistance and field. The coloring scheme is the same as in parts (a) and (b). When the field is low (high), the resistance is low (high) as well. When the field is at the transition, a bimodality can be seen. There is no resistance state in between the top and bottom resistances of the step.

IV. DISCUSSION

Superconducting systems subject to a uniform current distribution and in the presence of artificial periodic pinning exhibit minima in the magnetoresistance at matching fields due to the commensurability of the vortex lattice with the artificial pinning centers.[20] On the contrary, the bimodality of the steps and the increased resistance at low temperatures observed here suggest that vortex dynamics in the Corbino geometry has a different origin. However, the occurrence of steps at the matching fields implies that they are still related to the pinning sites.

Earlier studies of the Corbino geometry of superconductors with naturally occurring, random pinning showed that the gradient in the Lorentz and friction forces cause shearing of the vortex lattice.[13,21,22] Using molecular dynamics simulations, it was demonstrated that for increasing currents the vortex distribution undergoes a shearing transition from an elastic, through a plastic, to a laminar state.[22] Characteristic jumps in the resistance versus current accompany these shearing transitions. In the elastic state, the vortices move coherently as a rigid solid with the same angular velocity, while in the plastic state, dislocations, created in the region with highest strain, move along crystallographic directions. In the laminar state, the vortices move in annular channels with a $1/r$ angular velocity profile. Transport measurements on a YBCO device in the Corbino geometry show that at low temperatures, the vortex lattice is in an elastic state, whereas at high temperature the vortex lattice has a velocity distribution that corresponds to a plastic or laminar state.[13] These results were confirmed in a theoretical study using a mean field approach (Frenkel-Kontorova model).[21] With increasing temperature, the vortex lattice shears into two solid, concentric rings with different angular velocities. These two rings are connected by a laminar transition region in which the vortices move in annular channels (see Fig. 4 in Ref. 21). The elastic vortex lattice shears at the radius with the largest strain. This radius

is given by $r = \sqrt{R1 \times R2}$, where $R1$ is the inner and $R2$ the outer radius of the vortex distribution.[21]

In the studies presented here, as the magnetic field is raised, a stepwise increase is observed in the magnetoresistance of the inner region between contact I_+ and V_1 [Fig. 2(b)], while the magnetoresistance of the middle ring between contacts V_1 and V_2 remains zero. From this, we can infer that the vortex distribution consists of an outer part with fixed (pinned) vortices and an inner part with moving vortices. The mean field model[21] agrees that in our case the vortex distribution consists of two concentric rings separated by a very narrow laminar or plastic transition region. For the Corbino geometry under investigation, the inner and outer radii are 5 μm and 50 μm, respectively. According to the equation above, the radius of maximum strain would be approximately 16 μm. Hence, the laminar transition region would be inside the inner region, in agreement with the low temperature magnetoresistance measurements. The steps in the magnetoresistance curve might arise from an abrupt shearing of the inner solid ring caused by the commensurability of the vortex distribution with the artificial pinning centers. Little Parks oscillations in a superconducting wire network can be excluded. The Little Parks oscillations of the critical temperature are observed very close to T_C, while steps in the magnetoresistance were measured considerably below T_C. According to Ref. 21, the width of the laminar transition region increases, and the radius of the inner solid ring decreases with increasing temperature. This is in agreement with the decrease of step height that is observed for increasing temperatures [see Figs. 2(b) and 3(a)]. As the temperature is increased further, the influence of the inner solid ring on the magnetoresistance diminishes, and the laminar transition region becomes dominant. This results in the characteristic-matching minima [see Fig. 2(b) at $T/T_C = 0.998$]. At these temperatures, the laminar transition region significantly protrudes into the middle ring, and consequently matching minima can be observed in the magnetoresistance curve of the middle ring as well [Fig. 2(a)]. It is important to note that according to Ref. 23, the laminar state in a sheared vortex lattice is different from the laminar state induced by thermal fluctuation. In the sheared laminar state, polycrystallinelike order is preserved. Consequently, matching effects in a sheared laminar vortex lattice are plausible.

The details of the mechanism responsible for the bimodal steps remain elusive, and further studies are necessary. An important clue is presented in Fig. 3(b). Although the current is increased by one order of magnitude, the step sizes only doubles. Additionally, the fact that the steps are exactly at the matching fields implies that the commensurability with the pinning sites combined with the shearing induced by the current gradient is responsible for the steps.

In the mean field model,[21] the radial movement of dislocations is ignored, which makes it impossible to describe a plastic state within this framework. Therefore, a detailed understanding of the plastic vortex state (as described in Ref. 22) interacting with the pinning sites might be necessary to interpret the results of this study in detail, and a molecular dynamics simulations of a vortex lattice in a Corbino disc interacting with pinning sites would be very helpful. The three-point configuration that was used for the resistance measurements of the inner ring may have parasitic resistance, and we cannot exclude unknown resistive effects in the vicinity of the current injection. However, we assume that these are not contributing to the characteristics in the magnetoresistance curve for three reasons. First, for high temperature close to T_C, the magnetoresistance of the inner ring is qualitatively similar to the magnetoresistance of the middle ring, which was measured in a four-point configuration. Second, although the characteristic jumps appear only in the magnetoresistance of the inner ring, they are at the matching field. This indicates that they are related to the artificial pinning sites. Third, the jumps evolve gradually from the matching minima, hence, they probably have the same origin.

V. CONCLUSIONS

The vortex dynamics of superconductors under the influence of a periodic pinning lattice are measured in the Corbino geometry. At high temperatures, matching minima from the pinning lattice are found at the predicted magnetic fields. Surprisingly, at low temperatures the matching fields show steps rather than minima. The steps are bimodal with no state in between the two levels. The data indicates that these steps are due to a shearing transition in the elastic vortex lattice. The transition causes an increase in the angular velocity of the inner sheared area, which in turn causes a step in the voltage. This research shows that it is possible to control the shearing field with the proper choice of underlying pinning lattice.

ACKNOWLEDGMENTS

We thank Cynthia and Charles Reichhardt, Daniel Arovas and Sebastián Díaz for useful discussions. The National Science Foundation Grant No. DMR-0800207 funded the superconducting aspects of this work, whereas the lithography was supported by a grant from the U.S. Department of Energy under Grant No. DE FG03-87ER-45332.

[1] B. Haskell, P. M. Pizzochero, and S. Seveso, Astrophys. J. **764**, L25 (2013).
[2] C. F. Driscoll, D. Z. Jin, D. A. Schecter, and D. H. E. Dubin, Physica C **369**, 21 (2002).
[3] A. Eddi, A. Decelle, E. Fort, and Y. Couder, Europhys. Lett. **87**, 56002 (2009).
[4] K. Kadowaki, Sci. Technol. Adv. Mater. **6**, 589 (2005).
[5] D. S. Fisher, M. P. A. Fisher, and D. A. Huse, Phys. Rev. B **43**, 130 (1991).
[6] H. F. Hess, R. B. Robinson, R. C. Dynes, J. M. Valles, Jr., and J. V. Waszczak, Phys. Rev. Lett. **62**, 214 (1989).
[7] E. Altshuler, T. H. Johansen, Y. Paltiel, P. Jin, K. E. Bassler, O. Ramos, Q. Y. Chen, G. F. Reiter, E. Zeldov, and C. W. Chu, Phys. Rev. B **70**, 140505 (2004).

[8]E. R. Nowak, O. W. Taylor, L. Liu, H. M. Jaeger, and T. I. Selinder, Phys. Rev. B **55**, 11702 (1997).
[9]I. Giaever, Phys. Rev. Lett. **15**, 825 (1965).
[10]D. Perez de Lara, M. Erekhinsky, E. M. Gonzalez, Y. J. Rosen, I. K. Schuller, and J. L. Vicent, Phys. Rev. B **83**, 174507 (2011).
[11]C. J. Olson Reichhardt and C. Reichhardt, Phys. Rev. B **81**, 224516 (2010).
[12]M. Shaw and P. Solomon, Phys. Rev. **164**, 535 (1967).
[13]D. López, W. K. Kwok, H. Safar, R. J. Olsson, A. M. Petrean, L. Paulius, and G. W. Crabtree, Phys. Rev. Lett. **82**, 1277 (1999).
[14]P. Benetatos and M. C. Marchetti, Phys. Rev. B **65**, 134517 (2002).
[15]N. S. Lin, T. W. Heitmann, K. Yu, B. L. T. Plourde, and V. R. Misko, Phys. Rev. B **84**, 144511 (2011).
[16]N. S. Lin, V. R. Misko, and F. M. Peeters, Phys. Rev. B **81**, 134504 (2010).
[17]S. Okuma, Y. Tsugawa, and A. Motohashi, Phys. Rev. B **83**, 012503 (2011).
[18]A. Hoffmann, P. Prieto, V. Metlushko, and I. K. Schuller, J. Superconduct. Novel Magn. **25**, 2187 (2012).
[19]A. Daire, W. Goeke, and M. A. Tupta, *White Paper: New Instruments Can Lock Out Lock-ins* (Keithley Instruments, Inc., Cleveland, Ohio, 2005).
[20]Y. Jaccard, J. I. Martin, M.-C. Cyrille, M. Velez, J. L. Vicent, and I. K. Schuller, Phys. Rev. B **58**, 8232 (1998).
[21]A. Furukawa and Y. Nisikawa, Phys. Rev. B **73**, 064511 (2006).
[22]M.-C. Miguel and S. Zapperi, Nat. Mater. **2**, 477 (2003).
[23]M. Carmen Miguel, A. Mughal, and S. Zapperi, Phys. Rev. Lett. **106**, 245501 (2011).